Available online at www.sciencedirect.com
ScienceDirect
Journal of Molecular Catalysis A: Chemical 281 (2008) 24–34
JOURNAL OF MOLECULAR CATALYSIS A: CHEMICAL
www.elsevier.com/locate/molcata

# Study of the "explosive" NO + CO reaction on a Pt(1 0 0) surface by dynamic Monte Carlo simulation

S.J. Alas [a,b,*], L. Vicente [a]

[a] *Departamento de Física y Química Teórica, Facultad de Química, UNAM, 04510 México, D.F., Mexico*
[b] *Departamento de Química, Universidad Autónoma Metropolitana, Iztapalapa, P.O. Box 55-534, México, D.F., Mexico*

Available online 1 August 2007

**Abstract**

The so-called "surface explosion" observed through TPR experiments in the catalytic reduction of NO by CO on a Pt(1 0 0) surface is studied by using a dynamic Monte Carlo method on a square lattice at low pressure conditions. This analysis takes into account recent experimental evidences concerning the above reaction on a Rh(1 1 1) surface; such experiments have shown that the $N_2$ production occurs either from the classical N + N recombination step or by the formation and successive decay of a (N–NO)* intermediary species, being the last step the fastest pathway. Moreover, the effect on NO dissociation rate, i.e., the limiting step during the whole reaction, is inhibited by co-adsorbed NO and CO molecules and is enhanced both by the presence of empty sites and adsorbed N atoms as nearest-neighbors. In these simulations the experimental parameter values are included, such as adsorption, desorption and diffusion rates of the reactants. The "explosive" phenomenon is studied in the temperature range of 300–550 K. In our results, as the surface is totally covered with the adsorbates, cellular structures are observed.


*Keywords:* NO reduction; Surface explosion; Reaction fronts; Dynamic Monte Carlo simulation

## 1. Introduction

The catalytic reduction of NO by CO on the surface of noble metals has been studied during the past few years, both from experimental and theoretical points of view. This is due to the importance of this reaction in the problem of air pollution, especially for controlling the processes related to the decrease of $NO_x$ emissions [1,2]. Platinum metal has been successfully used to carry out this reaction, given that some of the Pt crystallographic planes are very efficient for NO dissociation, which is the limiting step for $CO_2$ formation. Within these Pt planes, the (1 0 0) and (1 1 0) surfaces are notably useful [3].

Particularly the NO + CO reaction taking place on a Pt(1 0 0) surface, in addition to its environmental importance, has a intrinsic fundamental interest, due to the fact that this reaction presents nonlinear phenomena such as kinetic oscillations, spatiotemporal pattern formations and chaotic behaviors within pressure and temperature ranges of around $10^{-6}$ to $10^{-4}$ Pa and 390–490 K, respectively [3–9].

It is well known that the clean Pt(1 0 0) surface, in its stable state, exhibits a reconstructed quasi-hexagonal configuration (hex) of the atoms located in the topmost layer, which can be reversibly lifted by the adsorption of molecules such as CO and NO thus leading to the formation of a (1 × 1) square structure. This constitutes an adsorbate-induced surface phase transition (SPT) of the type hex $\leftrightarrows$ 1 × 1, which is controlled by critical adsorbate coverages [3–10]. This SPT, at $T > 430$ K, participates directly in the oscillatory mechanism during the course of the NO +CO reaction [3,6–9]. Whereas at $T < 420$ K the hex $\leftrightarrows$ 1 × 1 phase transition is not essential to observe oscillations since the surface maintains its 1 × 1 structure. Therefore, in the NO + CO reaction over the Pt(1 0 0) surface, at low temperature conditions, the formation of the oscillatory patterns occurs by a periodic sequence of an autocatalytic "surface explosion" and by the restoration of an adsorbate-covered surface [6,10]. This explosive phenomenon has been observed during temperature programmed desorption (TPD) [11] and temperature programmed reaction (TPR) [6,12] experiments, and takes place when the Pt(1 0 0) surface undergoes a change between a state with a low catalytic activity, where a high-adsorbate coverage inhibits the dissociation of adsorbed NO molecules, and a state with a high-catalytic activity, where a low surface coverage allows NO dissociation to occur [6].

* Corresponding author at: Departamento de Física y Química Teórica, Facultad de Química, UNAM, 04510 México, D.F., Mexico.
*E-mail address:* espectros7@gmail.com (S.J. Alas).

1381-1169/$ – see front matter © 2007 Elsevier B.V. All rights reserved.
doi:10.1016/j.molcata.2007.07.043

The classical mechanism of NO reduction by CO over Pt(1 0 0) that has been employed to explain the formation of oscillations and the so-called "surface explosion" phenomenon consists of the following reaction steps:

$$CO_{(gas)} + \text{site} \leftrightarrows CO_{(ads)} \quad (1)$$

$$NO_{(gas)} + \text{site} \leftrightarrows NO_{(ads)} \quad (2)$$

$$NO_{(ads)} + \text{site} \rightarrow N_{(ads)} + O_{(ads)} \quad (3)$$

$$N_{(ads)} + N_{(ads)} \rightarrow N_{2(gas)} + 2\,\text{sites} \quad (4)$$

$$NO_{(ads)} + N_{(ads)} \rightarrow N_2O_{(gas)} + 2\,\text{sites} \quad (5)$$

$$CO_{(ads)} + O_{(ads)} \rightarrow CO_{2(gas)} + 2\,\text{sites} \quad (6)$$

In the reaction step (4), we can observe that the production of $N_{2(gas)}$ takes place through the recombination of two adsorbed N atoms located at two nearest-neighbor (nn) sites. The formation of the products of this reaction is directly related to the NO dissociation rate, since this rate is the step that is limiting the complete reaction [6,8,10].

Besides of this reaction mechanism, several other mechanisms have been proposed to explain the kinetic behavior of the NO + CO reaction over diverse surface types. One of these mechanisms that is reported in the literature corresponds to the formation of $N_2$ through the combination of $NO_{(ads)}$ and $N_{(ads)}$ as an alternative reaction pathway in the overall reaction scheme [13–23]. For example, Cho [19] proposed a mechanism where $N_2$ is produced via the formation of a surface $N_2O$ species, whose formation was demonstrated by early studies involving Rh supported on silica [15] and TPD studies on Rh(1 1 1) by the General Motors research group. Kortlüke and Von Niessen [20,21] assumed the NO + N recombination step as a possibility when studying the reaction on square and triangular lattices. Denton et al. [22] showed that the $N_2O$ is an intermediate for NO reduction into $N_2$ over Pt, during selective catalytic reduction (SCR) experiments, in stationary and transient conditions. Moreover, investigations made by Granger et al. [23] showed that during $N_2$ production an $N_2O$ alternative step could be involved during the reduction of NO by CO over noble metals.

In the past decade, Belton et al. [24] studied in detail the reduction of NO by CO on the Rh(1 1 1) surface, and they came to the conclusion that in this reaction at ultra high vacuum (UHV) conditions, at least over Rh(1 1 1), $N_{2(gas)}$ is exclusively formed by the recombination of two $N_{(ads)}$ and $N_2O_{(gas)}$ is formed by the reaction between $NO_{(ads)}$ and $N_{(ads)}$. Therefore, the last mechanism has been accepted for the same reaction occurring on both Pt(1 0 0) and Rh(1 1 1) surfaces. However, recent molecular beam experiments and theoretical studies performed by Zaera et al. [25–31] with respect to the reduction of NO over Rh(1 1 1) have indicated that the standard reaction scheme used to explain the kinetics of this reaction requires modification in at least two important ways. First, it was found that when a $^{14}N$-covered Rh(1 1 1) surface is exposed to a $^{15}NO$ + CO beam, the majority of molecular nitrogen produced contains at least one $^{15}N$ atom [25–27]. This means that the nitrogen recombination step, $N_{(ads)} + N_{(ads)} \rightarrow N_{2(gas)} + 2$ sites, usually assumed as responsible of the formation of molecular nitrogen is in fact not fast enough under typical reaction conditions to account for the $N_2$ production rate. Instead, an intermediate species, (N–NO)*, appears to be formed on the surface, and then either it decompose to $N_{2(gas)} + O_{(ads)}$, or it just simply desorbs. In a realistic description of the reaction mechanism, both the nitrogen recombination step and the formation of the (N–NO)* intermediary should be considered in parallel, the last one being the dominant step [31,32]. A second important modification to the typical NO reduction mechanism brought about by molecular beam work arises from the evidence that, at least for the case of Rh(1 1 1), atomic N forms compact islands on the surface. Indeed, it was found that the isotopic distribution of molecular nitrogen detected by TPD spectra from surfaces exposed to isotopic mixtures of $^{14}N$- and $^{15}N$-labeled nitrogen oxide could only be explained on that basis [28,30]. The mechanism for the formation of these islands, however, has hitherto not been established.

On the other hand, Niemantsverdriet and co-workers [33] found experimentally that NO dissociation is inhibited by the presence of neighboring co-adsorbed NO or CO species during the NO + CO reaction on Rh(1 1 1). They also detected that NO dissociation is facilitated by the existence of several nn vacant sites. The inhibition effect on NO dissociation is of fundamental importance; in fact, it was shown to be absolutely necessary in order to explain the negligible O coverage observed experimentally at steady-state conditions for low CO concentrations in the gas phase [32].

Recently, it has already been suggested that the alternative reaction mechanism observed by Zaera et al. for Rh(1 1 1) could also be valid for other surfaces such as Pt(1 0 0) where the hex $\leftrightarrows$ 1 × 1 phase reconstruction takes place [34–36]. For example, in a previous study this alternative mechanism and the effect of the inhibition of NO dissociation on Pt(1 0 0) was considered [36], as it was mentioned in the preceding paragraph. Moreover, the study carried out in [36] was also based on the experimental observations obtained by Fink et al. [10], where the NO dissociation is also inhibited by the existence of CO and NO molecules as nn on the Pt(1 0 0) surface. Although, there is no direct experimental evidence for the occurrence of an alternative mechanism on Pt(1 0 0), it is also true that there is no direct experimental evidence for the contrary. Even though, the arguments in favor to include an alternative reaction mechanism on NO dissociation and other related processes on Pt(1 0 0) can be reinforced by the DFT calculations developed by Neurock et al. [37,38].

It is therefore natural, in order to advance toward a realistic model for this reaction, to incorporate the above information emerging from the mentioned experimental studies into the reaction scheme and evaluate the effects of each factor. Given that the slow step of the catalyzed NO + CO reaction corresponds to the NO dissociation, the possibility of $N_2$ production through both the formation of the (N–NO)* intermediary and of the classical adsorbed N + N atoms recombination, as well as the formation of N-islands and the inhibition effect on NO dissociation by co-adsorbed NO or CO molecules, should be taken into account in the reaction model. In spite of that in a prior study [36] it was found that the formation of N-islands is of little importance to

account for oscillations due to the fact that adsorbed N atoms are rapidly removed from the surface, in this work this N-island formation is included in order to achieve a more complete model.

The purpose of the present work is to describe the kinetic evolution of the NO + CO/Pt(1 0 0) system during the so-called "surface explosion" phenomenon observed in TPR experiments by choosing the appropriate temperature-dependent rates for the majority of the elementary steps involved in the mechanism of reaction. This is made by means of the dynamic Monte Carlo simulation with a time evolution determined by reported experimental values for the rates of the elementary processes. Specifically, we will apply the dynamic simulation technique to the NO + CO reaction on Pt(1 0 0) by considering alternative steps in the reaction mechanism that surge after taking into account the experimental findings of Zaera et al., i.e., the production of $N_2$ via the (N–NO)* and N + N pathways and the formation of N-islands, as well as the contributions to the NO dissociation by Fink et al. [10] and Niemantsverdriet and co-workers [33]. We will discuss under which conditions the "surface explosion" and spatial patterns can be observed during this phenomenon and identify which are the dominant physicochemical processes that determine the occurrence of such behavior. In Section 2, we describe the details of the model and simulation method. Section 3 contains the results and the discussion about the simulations on a square lattice. Finally, the conclusions are presented in Section 4.

## 2. Model and simulation method

In our model, the surface of a Pt(1 0 0) single crystal is represented as a regular 2D square lattice with periodic boundary conditions. The lattice consists of L × L sites; a site indicates one Pt surface atom and each site has four neighbors. The gas phase is assumed to be a mixture of NO and CO molecules with partial pressures $p_{NO}$ and $p_{CO}$, respectively. Our reaction scheme takes into account the following assumptions:

(a) The formation of an (N–NO)* intermediary species as the principal step for the $N_2$ production,
(b) The production of $N_2$ via the classical N + N recombination step,
(c) The inhibition of NO dissociation due to the presence of neighboring co-adsorbed CO and NO particles,
(d) The enhancement of the NO dissociation rate by the presence of nn co-adsorbed N atoms (effect of N-island formation) and nn vacant sites,
(e) The desorption of NO and CO species, and
(f) The surface diffusion of NO and CO molecules.

For the dynamic analysis of the reduction of NO by CO on the Pt(1 0 0) surface, the alternative reaction scheme can be written as follows:

$$CO_{(gas)} + \text{site} \leftrightarrows CO_{(ads)} \quad (7)$$

$$NO_{(gas)} + \text{site} \leftrightarrows NO_{(ads)} \quad (8)$$

$$NO_{(ads)} + \text{site} \rightarrow N_{(ads)} + O_{(ads)} \quad (9)$$

$$NO_{(ads)} + N_{(ads)} \rightarrow (N\text{–}NO)^* + \text{site} \quad (10)$$

$$(N\text{–}NO)^* \rightarrow N_{2(gas)} + O_{(ads)} \quad (11)$$

$$N_{(ads)} + N_{(ads)} \rightarrow N_{2(gas)} + 2\,\text{sites} \quad (12)$$

$$CO_{(ads)} + O_{(ads)} \rightarrow CO_{2(gas)} + 2\,\text{sites} \quad (13)$$

$$NO_{(ads)} + \text{site} \rightarrow \text{site} + NO_{(ads)} \quad (14)$$

$$CO_{(ads)} + \text{site} \rightarrow \text{site} + CO_{(ads)} \quad (15)$$

In this reaction scheme, it can be observed that the conventional N + N recombination step (step (12)) has been included, as well as an alternative step involving the formation of an (N–NO)* intermediate species (steps (10) and (11)) for the production of $N_2$. The former pathway (step (12)) is slower than the latter one (steps (10) and (11)) and, according to Refs. [32,36], it will happen with a relative probability of 0.3, while that for the (N–NO)* pathway will be 0.7. Both the inhibition of NO dissociation by the co-adsorbates and the formation of N-islands will be suitably taken into account below when the NO dissociation rate will be determined. We also consider that diffusion of adsorbed NO and CO species can take place on the surface, as it is indicated in steps (14) and (15).

In order to count with a relatively simple and manageable reaction scheme, we incorporate the following additional assumptions in devising our surface reaction mechanism:

(i) The production of $N_2O$ gas phase is not taken into account, since the rate of this reaction step is expected to be slow compared with those corresponding to $CO_2$ and $N_2$ production [4,6,10].
(ii) Lateral interactions among different ad-species suggested by experimental studies are not considered here in the usual way, the effects of these interactions on the Pt(1 0 0) surface form c(2 × 2) and c(2 × 4) rearrangements [10,39–42]. In this work, lateral interactions can be considered in an indirect way due to the following reasons: first, the experimentally observed inhibition effects of co-adsorbed NO and CO species on the NO dissociation cannot be easily taken into account by the usual lateral interactions, but instead these can be taken into account by properly modifying the NO dissociation rate. Even if, the N-islands formation on Pt(1 0 0) is of small significance, in this study we assume a kinetic mechanism for the formation of these islands, that is, NO dissociation is favored by the presence of adsorbed N atoms.
(iii) Oxygen desorption is neglected as experiments have shown that this process occurs at temperatures above 600 K [10,40,43]. In our simulations, we varied the temperature in the range of 300–550 K; therefore, adsorbed O atoms are removed from the surface only by their reaction with CO.
(iv) Oxygen atoms diffusion is neglected, as this process is expected to be slower than the remaining reaction steps. This is because oxygen atoms are strongly bonded to the surface [44,45].
(v) The diffusion of N atoms is not included, since its diffusion constant value is several orders of magnitude smaller than

those of the CO and NO molecules [45]. Moreover, in this reaction scheme $N_2$ is mainly produced through the formation and decomposition of an (N–NO)* intermediary species and since NO diffusion is allowed, therefore, N and NO species can easily meet at two nn sites; in contrast with the classical reaction scheme where $N_2$ is only formed through the recombination of two adsorbed N atoms and N diffusion is strictly required [9,46].

In our model, the time evolution of the system is assumed to occur as a Markovian stochastic process. Under such scheme, every elementary reaction step has a rate constant associated with the probability per unit time for the occurrence of such step. A master equation describes the time evolution of the probability distribution of the states of the physical systems [47]:

$$\frac{\partial P_\alpha(t)}{\partial t} = \sum_\beta [W_{\beta\to\alpha} P_\beta(t) - W_{\alpha\to\beta} P_\alpha(t)] \tag{16}$$

Here, $P_\alpha(t)$ and $P_\beta(t)$ are the probability to find the system in given configurations $\alpha$ and $\beta$, respectively, at time $t$, and can be considered as components of a vector $P$ representing the probability distribution of the whole set of system configurations, and $W$ is the transition probability per unit time of the different processes indicated as subscripts.

This master equation can be simulated through a dynamic Monte Carlo technique. The simulation can be performed through the "random selection method", which can be adapted to our system as follows:

(i) A surface site is selected at random with probability $1/N$; where $N$ indicates the total number of sites existing at the moment.
(ii) A given $i$-type reaction step (i.e., desorption, diffusion, etc.) is chosen at random with probability $W_i/R$, where $R$ is the sum of the rates of all possible processes (with the exception of adsorption), i.e., the total-transition rate constant of the system.
(iii) If the selected $i$-type reaction step is viable (according to certain rules to be specified below) on the chosen site, then it is immediately executed.
(iv) After a given site is selected, the time is increased by $\Delta t$ according to

$$\Delta t = -\frac{\ln \xi}{NR} \tag{17}$$

where $\xi$ is a random number selected according to a uniform probability distribution in the interval (0,1). This equation renders the real time evolution caused by a system transition.

In our simulations the TPR studies are analyzed by means of the next algorithm:

(i) We fix $T = T_0$, where $T$ is the absolute temperature and $T_0$ is the initial absolute temperature.
(ii) We chose at random either a CO or an NO molecule from the gas phase.
(iii) When the surface reaches a certain coverage of adsorbed CO and NO molecules, we fix $\theta = \theta_0$ ($N = N_0$); where $\theta_0$ is the initial coverage and $N_0$ is the initial total number of occupied sites.
(iv) We select a random number between 0 and 1, and the time is increased according to Eq. (17).
(v) When $\Delta t$ is approximately 1 s, the temperature changes as $T = T_0 + \beta\Delta t$, where $\beta$ is the heating rate.
(vi) $N$ and $\theta$ are updated.
(vii) This process is repeated from step (iv) until the system reaches a given temperature.

The main elementary reaction steps and their corresponding rate constants are taken into account in the simulation scheme as follows.

### 2.1. Adsorption

A molecule of CO or NO is chosen from the gas phase, according to the corresponding flux given by the Hertz–Knudsen equation:

$$J_i = \frac{p_i}{(2\pi m_i kT)^{1/2}} \tag{18}$$

where $J_i$ is the flux of NO or CO molecules in $m^{-2}\,s^{-1}$, $p_i$ the partial pressure of the $i$-type molecule, $m_i$ the mass of NO or CO, and $k$ is the Boltzmann constant. The adsorption rate $W_i$ of particles impinging on the surface per site and per second is then obtained as

$$W_i = J_i A S_0 \tag{19}$$

where $A$ is the area per site on the surface, in this case of Pt(1 0 0), and $S_0$ is the initial sticking coefficient.

### 2.2. Desorption

Desorption is considered as an activated process with a rate given by

$$W_i = \nu_i \exp \frac{-E_{ai}}{kT} \tag{20}$$

where $\nu_i$ is the frequency factor and $E_{ai}$ the activation energy for species $i$.

### 2.3. Diffusion

Diffusion jumps are allowed both for CO and NO species to vacant nn sites. The diffusion rate $W_i$ is obtained directly as a frequency factor $\nu_i$.

### 2.4. NO dissociation

On a Pt(1 0 0) surface this process can only occur with the availability of a vacant nn site. According to the experimental observations of NO dissociation and to the theoretical simulations in the NO + CO reaction on Rh(1 1 1) [6,10,31–33], the

dissociation of NO, being a complex and the most important process, deserves separate consideration. The following features are taken into account:

(a) NO dissociation is facilitated by the presence of nn co-adsorbed N atoms, i.e., the NO dissociation probability increases with the presence of nn N atoms, which is the mechanism we assume for the formation of N-islands.
(b) The NO dissociation rate increases with increasing number of vacant nn sites.
(c) The blocking effect on the NO dissociation probability is caused by the presence of neighboring co-adsorbed NO and CO molecules. Therefore, the following expression is proposed for the dissociation rate for a NO molecule located at a given site on the surface:

$$W_{\mathrm{NOdis}} = \frac{W_{\mathrm{NOidis}}(C_{\mathrm{N}}n_{\mathrm{N}} + C_{\mathrm{V}}n_{\mathrm{V}} - C_{\mathrm{NO}}(n_{\mathrm{NO}} + n_{\mathrm{CO}}))}{4} \quad (21)$$

Here $W_{\mathrm{NOidis}}$ is an "initial" dissociation rate calculated as an activated process, as in Eq. (20), with appropriate frequency factor and activation energy given in Table 1, $n_{\mathrm{N}}$ is the number of nn sites occupied by adsorbed N atoms, $n_{\mathrm{V}}$ is the number of nn empty sites, $n_{\mathrm{NO}}$ and $n_{\mathrm{CO}}$ are the number of nn co-adsorbed NO and CO species, respectively, and the coefficients $C$ are the corresponding weighting factors.

### 2.5. $N_2$ production

This reaction step can follow two alternative pathways: (a) through the formation of an intermediate (N–NO)* species when two nn sites are occupied by N and NO species, as it is indicated in the step (10), and this is immediately followed by step (11) to give $N_2$, with a probability 0.7; (b) through the recombination of two nn adsorbed N atoms, with a corresponding probability of 0.3. The $N_2$ rate is determined as an activated process, as in Eq. (20), with the appropriate frequency factor and activation energy.

### 2.6. $CO_2$ production

This process is possible when CO and O species occupy two nn sites. It is considered as an activated process.

## 3. Results and discussion

A large amount of simulations were performed trying to understand the effects of the different parameters on the overall kinetic behavior of the CO + NO/Pt(1 0 0) system. Here, we only show the most important results.

In our simulations the partial pressures of reactants in the gas phase are kept constant, that is, $p_{\mathrm{CO}} = 3.0 \times 10^{-5}$ Pa and $p_{\mathrm{NO}} = 4.0 \times 10^{-5}$ Pa, while the temperature changes in the range of 300–550 K, both conditions are similar to those used in actual experiments [6,10]. In addition to these pressures and temperatures, Table 1 shows the values of the remaining parameters that have been employed in order to obtain the rate of each elementary reaction step; experimental values of these parameters are also included for comparison. Since no available data exist for the decay of the (N–NO)* complex intermediate to $N_2$, and consequently for the value of the corresponding rate constant, we have instead employed for this assignment the experimental values of $N_2$ formation proceeding from the classical N + N recombination. The values of the weighting factors used in Eq. (21) will be kept fixed at $C_{\mathrm{N}} = 0.7$, $C_{\mathrm{V}} = 0.7$ and $C_{\mathrm{NO}} = 0.2$; the effects of these values have already been analyzed in Ref. [36].

In our study, the simulation of the NO + CO reaction on Pt(1 0 0) starts from a completely 1 × 1 clean surface, on which it is feasible to perform the adsorption of both CO and NO molecules in a $p_{\mathrm{CO}}$:$p_{\mathrm{NO}}$ = 3:4 ratio at 300 K in order to form a monolayer. When the surface reaches a certain initial coverage value $\theta_0 = \theta_{\mathrm{CO}} + \theta_{\mathrm{NO}}$, for instance $\theta_0 = 0.5$, the adsorption processes for catching more CO and NO molecules stop. Then the temperature starts to increase with a heating rate $\beta = 2\ \mathrm{K\ s^{-1}}$ and hereafter the other processes included in the simulation begin to take place. These are CO and NO desorption, NO dissociation, CO + O reaction, formation of the (N–NO)* intermediary species, N + N recombination reaction, and CO and NO diffusion. The simulations end when the temperature attains the value of 550 K. Within this temperature interval (300–550 K) the sys-

Table 1
Values of the parameters used in simulations and their comparison with their experimentally observed values. The experimental values can be consulted in Refs. [6,10]. Where $p$ is the partial pressure, $S_0$ the initial sticking coefficient, $\nu$ the frequency factor, and $E_{\mathrm{a}}$ is the activation energy

| Reaction | $p^{\mathrm{exp}}$ ($\times 10^{-5}$ Pa) | $p^{\mathrm{sim}}$ ($\times 10^{-5}$ Pa) | $S_0^{\mathrm{exp}}$ | $S_0^{\mathrm{sim}}$ |
|---|---|---|---|---|
| CO adsorption | 3.0 | 3.0 | ≈0.8 | 0.8 |
| NO adsorption | 4.0 | 4.0 | ≈0.8 | 0.8 |
| **Reaction** | $\nu^{\mathrm{exp}}$ ($\mathrm{s^{-1}}$) | $\nu^{\mathrm{sim}}$ ($\mathrm{s^{-1}}$) | $E_{\mathrm{a}}^{\mathrm{exp}}$ (kJ/mol) | $E_{\mathrm{a}}^{\mathrm{sim}}$ (kJ/mol) |
| CO desorption | $1.0 \times 10^{14}$ to $10^{15}$ | $1.0 \times 10^{14}$ | 148.6–157.0 | 157.0 |
| NO desorption | $1.7 \times 10^{14}$ to $10^{15}$ | $1.7 \times 10^{14}$ | 142.3–154.9 | 154.9 |
| NO dissociation | $2.0 \times 10^{15}$ | $2.0 \times 10^{15}$ | 119.3 | 119.3 |
| $N_2$ production | $1.3 \times 10^{11}$ | $1.3 \times 10^{11}$ | 84.6 | 84.6 |
| $CO_2$ production | $2.0 \times 10^{8}$ | $2.0 \times 10^{8}$ | 58.6 | 58.6 |
| CO diffusion | – | 0–30 | – | – |
| NO diffusion | – | 0–30 | – | – |

tem undergoes the phenomenon known as "surface explosion", i.e., the adsorbed NO and CO molecules react to form extremely narrow products peaks of $CO_2$ and $N_2$ during a very short period of time.

The first results obtained from our numeric simulations tried to mimic this "explosive" phenomenon, which has been observed through TPR experiments [6,12], are depicted in Figs. 1–3. Here, we consider the case where the diffusion of both CO and NO molecules are not included.

Fig. 1 shows the TPR spectra simulated for different initial coverages of a mixture of CO and NO molecules, obtained from an average of 20-run simulations on lattices with $1024 \times 1024$ sites. In Fig. 1(a), it is possible to visualize the TPR spectrum for the amount of desorbed particles per interval of temperature. Fig. 1(b) and 1(c) shows the production of $CO_2$ and $N_2$ molecules, respectively. In these three figures, it is observed that when the initial coverage is between 0.5 and 0.9 the peaks (maxima) of temperature are situated between 404 and 422 K, but if the initial coverage is 1.0 then the maxima are at 464 K. Table 2 shows a summary about the temperature maxima changes.

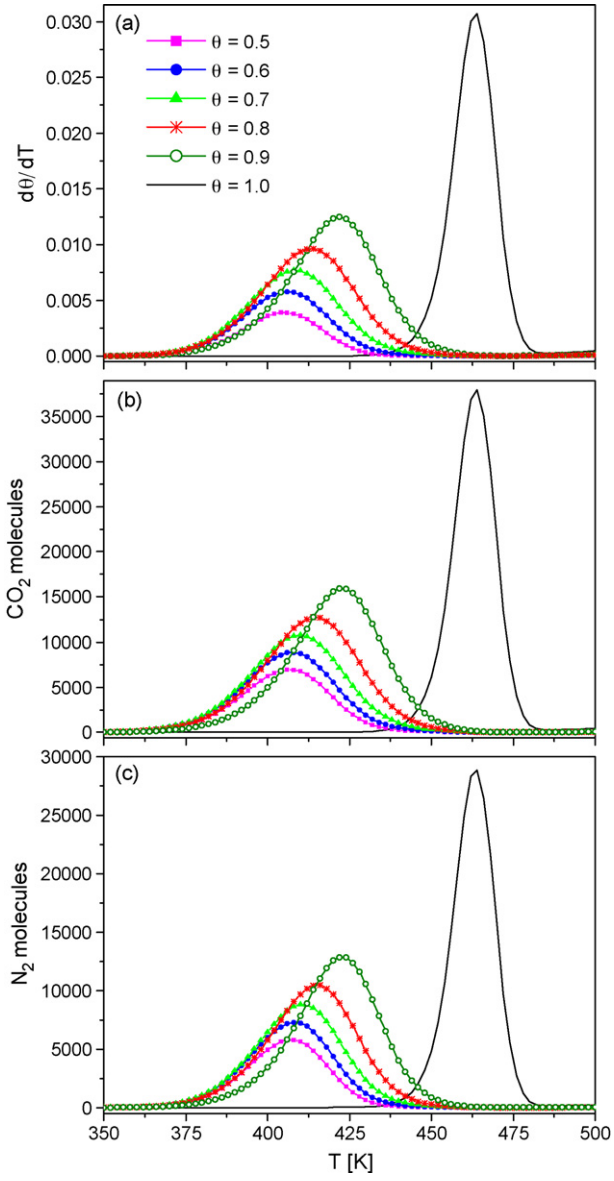


Fig. 1. Simulated TPR spectra: (a) amount of desorbed particles per interval of temperature; (b) production of $CO_2$ molecules; (c) production of $N_2$ molecules. Rates for $W_{COdif} = W_{NOdif} = 0\,s^{-1}$. Heating rate: $\beta = 2\,K\,s^{-1}$. Grid size: $1024 \times 1024$ sites.

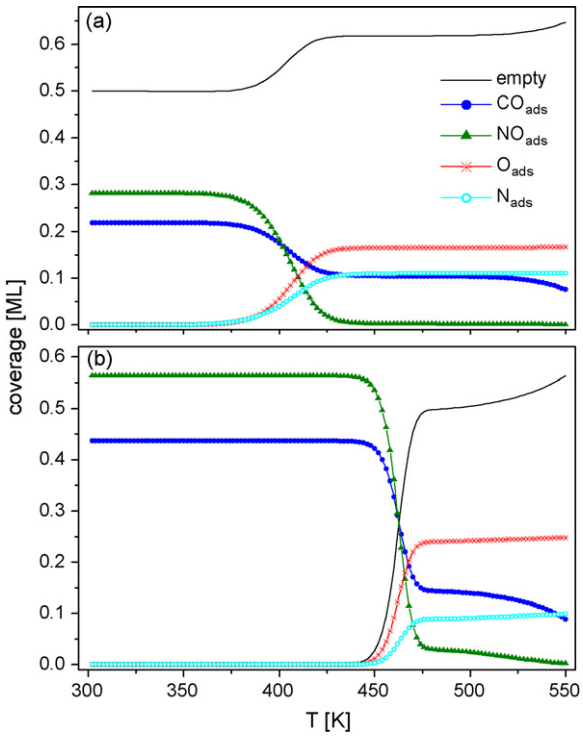


Fig. 2. Steady-state coverage for the simulated TPR spectra of Fig. 1 at two different initial coverages: (a) $\theta_0 = 0.5$; (b) $\theta_0 = 1.0$.

The above behaviors have the next explanations: when the initial coverage of the species is low ($\theta_0 = 0.5$), there are many empty sites on the surface and, as it was mentioned before, the presence of vacant sites enhance the possibility of NO dissociation. If a free site is next to an nn adsorbed NO molecule, then such molecule has the probability of dissociating into N and O atoms. Therefore, if this dissociation step is accomplished, the adsorbed O atom can then react with an adsorbed CO molecule while, in turn, the adsorbed N atom can also react with either an adsorbed NO molecule, thus forming the (N–NO)* complex intermediate, or with another adsorbed N atom. The species that are formed on the surface can desorb as $CO_2$ and $N_2$ toward the gas phase. New vacant sites are created on the surface

Table 2
Temperature maxima during TPR spectra simulations from different initial coverage values. NO and CO diffusion processes are neglected

| $\theta$ | Temperature (K) | | |
|---|---|---|---|
| | $d\theta/dT$ | $CO_2$ rate | $N_2$ rate |
| 0.5 | 404 | 406 | 406 |
| 0.6 | 406 | 408 | 408 |
| 0.7 | 408 | 410 | 410 |
| 0.8 | 414 | 414 | 416 |
| 0.9 | 422 | 422 | 422 |
| 1.0 | 464 | 464 | 464 |

thus allowing more adsorbed NO particles to dissociate; subsequently, more O and N atoms can continue reacting, leading to an autocatalytic "explosive" surface reaction. But, if the initial coverage value is large then increasing the amounts of CO and NO molecules on the surface, the NO dissociation is inhibited in consequence; therefore, CO/NO-islands are formed more frequently on the square phase. These attractive lateral interactions existing between the co-adsorbed CO and NO species provoke that the maxima of the TPR spectra being displaced to higher temperatures. When the surface is totally covered by CO and NO molecules, i.e., $\theta_0 = 1.0$, we can observe that the reaction peaks are located at a higher temperature value (464 K), this is because on the surface there are not empty sites and the reaction is locally inhibited by a high-adsorbate coverage, then NO dissociation can only occur when either a CO or NO molecule desorbs from the surface toward the gas phase. NO dissociation is delayed because the CO and NO desorption processes are slow, since the rate constants for these reaction steps are small; details can be consulted in Table 1.

Fig. 2 shows the steady-state surface coverage as function of temperature for each adsorbed species, measured in monolayers (ML); the empty site fractions are also shown in this figure. Fig. 2(a) corresponds to an initial coverage $\theta_0 = 0.5$; here it is possible to visualize that at about $T < 350$ K, the different coverages are almost constant, but when the temperature is increased, the adsorbed NO molecules start to dissociate into adsorbed N and O atoms. As more vacant sites are being generated by the reaction processes, NO is more likely to dissociate and as the temperature is gradually increased, the reaction rates are also enhanced, therefore the dissociation step becomes faster and the adsorbed species rapidly react. When the coverage of the adsorbed NO molecules decays toward zero, $T \approx 430$ K, there are remnants of CO, N and O particles on the surface due to the following situations: (a) NO molecules are initially in excess and produce many N and O atoms by dissociation, so that CO molecules cannot consume all adsorbed O atoms; (b) N diffusion is neglected, otherwise the surplus N atoms could react to form $N_2$ by the classical N + N recombination way; (c) in this section of the simulations study, NO and CO diffusions are not taken into account (these reactions steps will be discussed below). The steady-state represented in Fig. 2(b) stands for an initial coverage of 1.0. Here, it can be observed that the coverage behaviors and the creation of free sites are qualitatively the same as in Fig. 2(a), with the exception that in Fig. 2(b) the system presents a narrower reaction window around $T = 450$ K, than that found in Fig. 2(a).

Fig. 3 corresponds to a snapshot series of the surface covered with the different adsorbed particles and free sites, as the initial CO–NO coverage is $\theta_0 = 1.0$. Fig. 3(a) depicts, at 450 K, that the surface is almost totally covered by CO and NO molecules, but

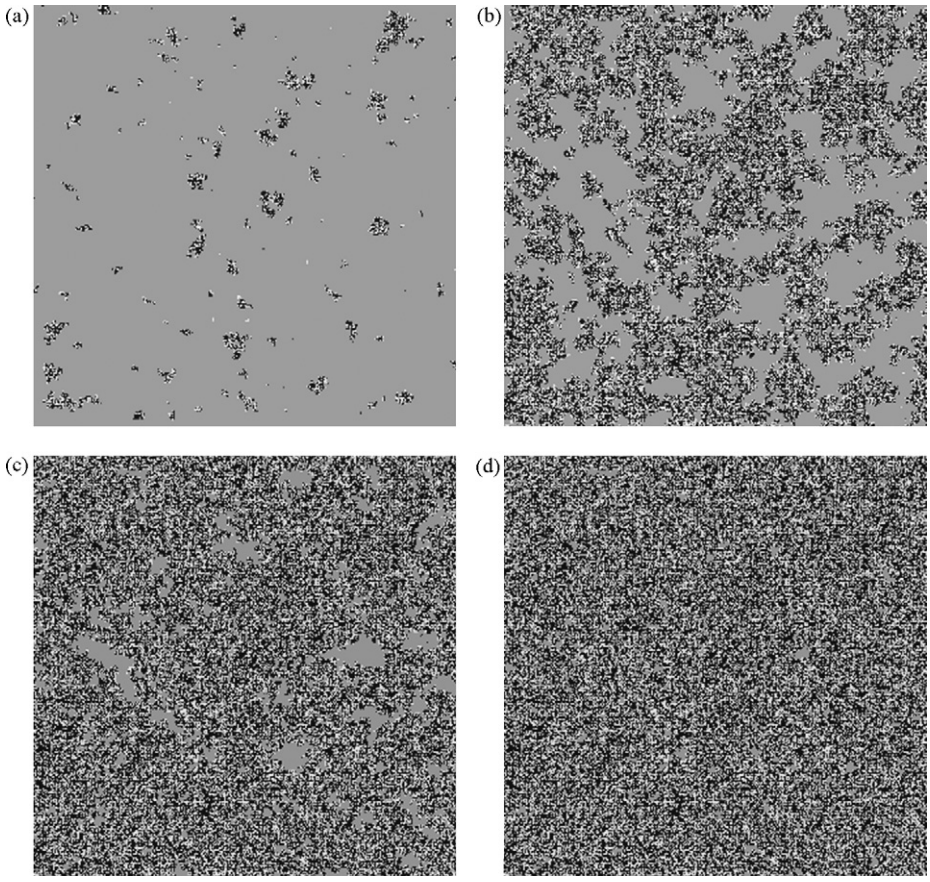


Fig. 3. Surface snapshots corresponding to the simulated TPR spectra when the initial coverage $\theta_0 = 1.0$ and the rates for $W_{COdif} = W_{NOdif} = 0\ s^{-1}$. Grey areas indicate adsorbed CO and NO molecules; black areas show adsorbed O and N atoms; and white areas are empty sites. A fragment of $512 \times 512$ sites of the whole lattice is herein shown.

it is possible to visualize that in some parts of the surface empty sites are being created by the desorption and subsequent reaction processes. Fig. 3(b) shows that, at 464 K, regions of empty sites start to grow and the adsorbed NO molecules have more opportunity to dissociate; therefore, the quantities of O and N atoms are also enhanced. This temperature corresponds to the maxima of the TPR spectra (cf. Fig. 1). When the temperature is further increased to 470 K, the CO and NO coverages decrease, whilst the O and N coverages and the amount of free sites increase, just as is indicated in Fig. 3(c). Finally, Fig. 3(d) shows a snapshot, at 490 K, when the reaction has ended; however, remnants of adsorbed CO, O and N particles still exist on the surface without reacting, in turn, NO molecules have totally dissociated or reacted.

On the other hand, when the processes of CO and NO diffusion are included in the simulations, with a rate constant of $10\,s^{-1}$ for both molecules, the following changes have been observed in the system behavior.

The temperature maxima of the simulated TPR spectra are located at lower values that those attained when the diffusion processes are not incorporated. In fact, when the initial coverage is between 0.5 and 0.9 the peaks are situated between 400 and 408 K (Fig. 4). These results are consistent with the experimental observations, since it has been observed that the "explosive" formation of $CO_2$ and $N_2$ occurs around 400 and 410 K [10,11]. However, when the initial coverage is increased to 1.0 then the temperature maxima can be found at 444 K. Fig. 4 shows these outcomes, whereas Table 3 shows the temperature maxima values for the different TPR spectra. As it can be observed if the initial coverages are between 0.5 and 0.9 the temperature peaks have a variation of 6 K, that is, the maxima are virtually independent of the initial coverage, which is in concordance with the experiments reported by Lesley and Schmidt [11]. These authors found that the $CO_2$ and $N_2$ products in the CO + NO reaction on Pt(1 0 0), desorb in the form of simultaneous sharp peaks around 410 K, which suggest that the sharp $CO_2$ and $N_2$ peaks are very nearly independent of the initial coverage. Fink et al. [10] have also reported by TPR experiments that the position and half-width of the $CO_2$ and $N_2$ product peaks around 400 K are almost independent of the initial coverage conditions. Moreover, in our simulations we have observed that when $\theta_0 > 0.7$ the $CO_2$ and $N_2$ product peaks show a half-width of around 13–22 K; this fact is in agreement with recent experimental TPR observations performed by Matveev et al. [12]. These authors have reported that the products ($CO_2$ and $N_2$) synchronously desorb in the form of sharp peaks with a half-width of 7–20 K.

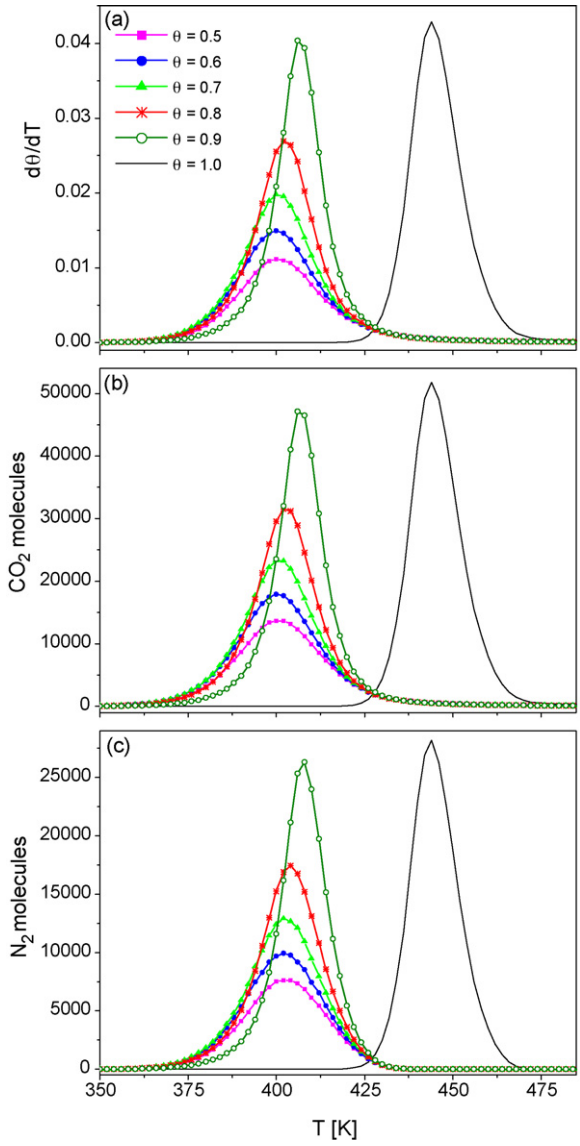


Fig. 4. Simulated TPR spectra: (a) amount of desorbed particles per interval of temperature; (b) production of $CO_2$ molecules; (c) production of $N_2$ molecules. Rates for $W_{COdif} = W_{NOdif} = 10\,s^{-1}$. Heating rate: $\beta = 2\,K\,s^{-1}$. Grid size: 1024 × 1024 sites.

Table 3
Temperature maxima during TPR spectra simulations from different initial coverage values. NO and CO diffusion processes are included, in this case $W_{COdif} = W_{NOdif} = 10\,s^{-1}$

| $\theta$ | Temperature (K) | | |
|---|---|---|---|
| | $d\theta/dT$ | $CO_2$ rate | $N_2$ rate |
| 0.5 | 400 | 400 | 402 |
| 0.6 | 400 | 400 | 402 |
| 0.7 | 400 | 400 | 402 |
| 0.8 | 402 | 402 | 404 |
| 0.9 | 406 | 406 | 408 |
| 1.0 | 444 | 444 | 444 |

The effect of CO and NO surface diffusion allows that the different adsorbed particles react faster; hence, the probability that NO molecules can dissociate into N and O atoms increase. Due to the mobility of the CO and NO molecules, these species are totally consumed or, in the case of NO, dissociated, as can be observed in Fig. 5. In Fig. 5(a) and (b), it is possible to visualize remnants of N and O atoms, while adsorbed CO and NO molecules are exhausted.

The system behavior deserves attention when the initial coverage is $\theta_0 = 1.0$. When either CO or NO desorption generates an empty site at random on the surface, an adsorbed NO molecule can dissociate and the atoms produced by this process can react. If the adsorbed N and O atoms react, with N or NO and CO,

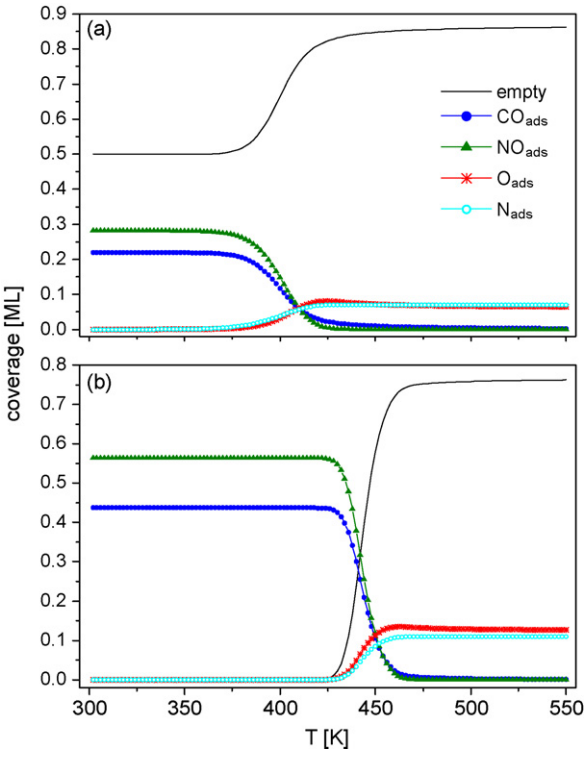


Fig. 5. Steady-state coverage for the simulated TPR spectra of Fig. 4 at two different initial coverages: (a) $\theta_0 = 0.5$; (b) $\theta_0 = 1.0$.

respectively, more vacant sites are created on the surface; in this way a reaction front is generated. Due to the fact that the adsorbed CO and NO molecules diffuse, the molecules at the front edge will diffuse toward the empty sites that have been formed inside the front, increasing in this manner the front size. Moreover, other reaction fronts can be generated at random on the surface. In this way, the diffusion of both species can spread the reaction fronts, thus originating spatiotemporal patterns, in this case cellular pattern types. This result is consistent with the experimental evidences, since CO and NO diffusion is necessary in order to observe pattern formations [5]. Fig. 6 illustrates the details related to the creation of reaction fronts in a lattice consisting of $1024 \times 1024$ sites. Fig. 6(a) shows the formation and growth of reaction fronts at 430 K. The reaction fronts start to spread across the surface at 436 K, as it is shown in Fig. 6(b). Fig. 6(c) depicts that, when these reaction fronts grow sufficiently in size, they star colliding against each other by reason of the boundary conditions and start to extinguish at 444 K; this temperature corresponds to the maximum of the TPR spectra shown in Fig. 4. Fig. 6(d) shows how the reaction fronts are almost completely extinguished at 450 K. Here, we can observe that N and O atoms remain adsorbed on the surface without reacting. Tammaro and Evans also reported analogous reaction fronts and their subsequent propagation for the NO + CO reaction on Pt(1 0 0) via the standard mean-field reaction-diffusion equations [46].

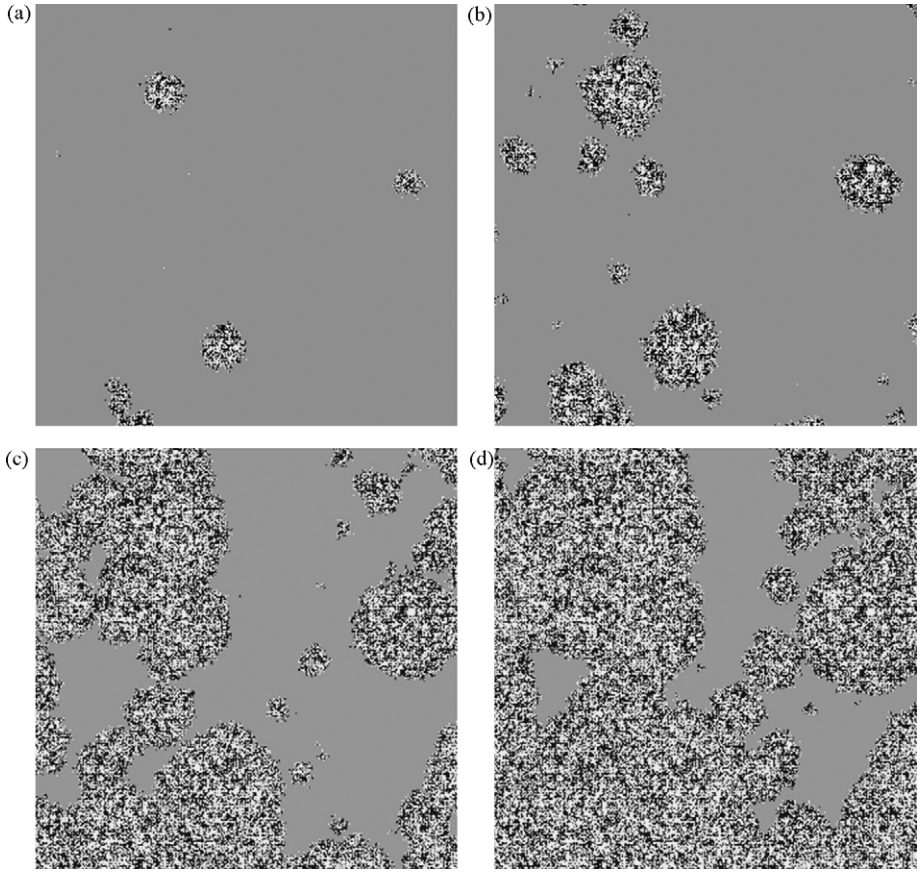


Fig. 6. Surface snapshots corresponding to the simulated TPR spectra when the initial coverage $\theta_0 = 1.0$ and the rates for $W_{COdif} = W_{NOdif} = 10\,s^{-1}$. The color code is the same as that employed in Fig. 3. A fragment of $512 \times 512$ sites of the whole lattice is herein shown.

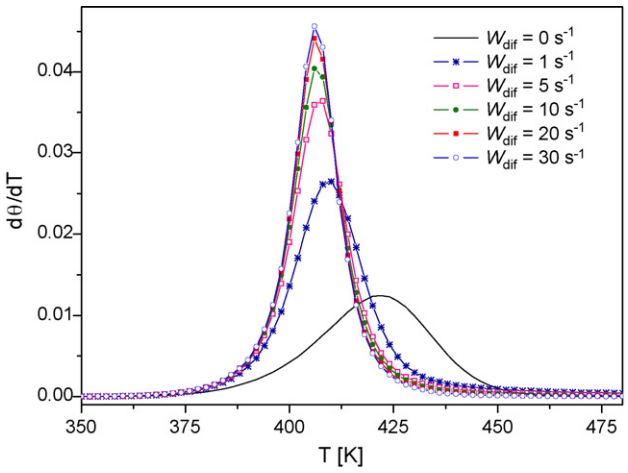


Fig. 7. Effect of CO and NO mobilities during the "surface explosion" occurring at $\theta_0 = 0.9$. Different values of $W_{dif} = W_{COdif} = W_{NOdif}$ are shown. Grid size: $1024 \times 1024$ sites.

Finally, Fig. 7 shows the effect created by increasing the diffusion rates, from $W_{dif} = 0$ to 30 $s^{-1}$, for $\theta_0 = 0.9$. From there, it can be observed that the maxima are shifted toward lower temperatures as $W_{dif}$ is increased. Note that for $W_{dif}$ values greater than 10 $s^{-1}$, the temperature values of the maxima generated during the "explosive" phenomenon attain a limiting value of $T = 406$ K. In contrast, the maximum for the non-diffusion case is around 422 K. Therefore, we have found in this work, that CO and NO surface diffusion processes are very important with respect to the surge and development of the "surface explosion" phenomenon. By taking into account the effect of surface diffusion allows us to reach an agreement between our calculations and the reported experimental values mentioned before [6,11,12].

## 4. Conclusions

We have studied by dynamic Monte Carlo simulations the "surface explosion" phenomenon during the NO + CO reaction on Pt(1 0 0) in the temperature range of 300–550 K and low pressures under the hypothesis that the reaction step leading to the formation of $N_2$ occurs not only through the classical N + N recombination step but, and more importantly, through the formation of a (N–NO)* intermediary species, as suggested by experiments performed on Rh(1 1 1). Additionally, other relevant experimental observations have been included in the present study regarding the NO dissociation rate, which is enhanced by the existence of co-adsorbed nn N atoms (i.e., effect of N-islands formation) and by the presence of nn vacant cells, whilst it is depressed by the presence of co-adsorbed nn NO and CO molecules.

The principal result of the present study is the appearance of an "explosive" behavior associated with the formation, in a natural way, of reaction fronts similar to cellular-like patterns. The visualization of these phenomena is possible when in the reaction mechanism model the main elementary steps are taken into account, namely: adsorption, desorption and diffusion of CO and NO molecules, NO dissociation, $CO_2$ and $N_2$ production through the formation of the (N–NO)* intermediary species, and the classical N + N recombination.

When we include the CO and NO surface diffusion processes, the temperature maxima in the $N_2$ and $CO_2$ production rates and desorbed particles per interval of temperature obtained from TPR simulations are in agreement with the experimental evidences if the initial coverage is between 0.5 and 0.9. Moreover, it is possible to observe the formation of reactions fronts when $\theta_0 = 1.0$.

In this study the formation of N-islands is not reported since this behavior is of small importance, as the production of $N_2$, via the formation of (N–NO)* intermediary species and by the N + N classical reaction, is fast. Moreover, an exhaustive study to this respect was already performed in a previous work [36].

## Acknowledgments

The authors would like to thank the financial support provided to Dr. S. de J. Alas G. by the Consejo Nacional de Ciencia y Tecnología (CONACyT, México) through project number 52880 and also acknowledge CONACYT 49968-F.

## References

[1] M.A. Gómez-García, V. Pitchon, A. Kiennemann, Environ. Int. 31 (2005) 445.
[2] F. Garin, Appl. Catal. A: Gen. 222 (2001) 183.
[3] R. Imbihl, G. Ertl, Chem. Rev. 95 (1995) 697.
[4] S.B. Schwartz, L.D. Schmidt, Surf. Sci. 206 (1988) 169.
[5] G. Veser, R. Imbihl, J. Chem. Phys. 96 (1992) 7155.
[6] Th. Fink, J.-P. Dath, R. Imbihl, G. Ertl, J. Chem. Phys. 95 (1991) 2109.
[7] G. Veser, F. Mertens, A.S. Mikhailov, R. Imbihl, Phys. Rev. Lett. 71 (1993) 935.
[8] G. Veser, R. Imbihl, J. Chem. Phys. 100 (1994) 8483;
G. Veser, R. Imbihl, J. Chem. Phys. 100 (1994) 8492.
[9] V.P. Zhdanov, Surf. Sci. Rep. 45 (2002) 231.
[10] Th. Fink, J.-P. Dath, M.R. Bassett, R. Imbihl, G. Ertl, Surf. Sci. 245 (1991) 96.
[11] M.W. Lesley, L.D. Schmidt, Surf. Sci. 155 (1985) 215.
[12] A.V. Matveev, A.A. Sametova, V.V. Gorodetskii, Kinet. Catal. 45 (2004) 598.
[13] V.P. Zhdanov, B. Kasemo, Surf. Sci. Rep. 29 (1997) 31.
[14] C.T. Campbell, J.M. White, Appl. Surf. Sci. 1 (1978) 347.
[15] W.C. Hecker, A.T. Bell, J. Catal. 84 (1983) 200.
[16] A. Chin, A.T. Bell, J. Phys. Chem. 87 (1983) 3700.
[17] P. Ho, J.M. White, Surf. Sci. 137 (1984) 103.
[18] T.W. Root, L.D. Schmidt, G.B. Fisher, Surf. Sci. 150 (1985) 173.
[19] B.K. Cho, J. Catal. 138 (1992) 255.
[20] O. Kortlüke, W. Von Niessen, J. Chem. Phys. 105 (1996) 4764.
[21] O. Kortlüke, W. Von Niessen, Surf. Sci. 401 (1998) 185.
[22] P. Denton, Y. Schuurman, A. Giroir-Fendler, H. Praliaud, M. Primet, C. Mirodatos, C.R. Acad. Sci. Paris, Série IIc, Chim. 3 (2000) 437.
[23] P. Granger, L. Delannoy, J.J. Lecomte, C. Dathy, H. Praliaud, L. Leclercq, G. Leclercq, J. Catal. 207 (2002) 202.
[24] D.N. Belton, C.L. DiMaggio, S.J. Schmieg, K.Y.S. Ng, J. Catal. 157 (1995) 559.
[25] F. Zaera, C.S. Gopinath, J. Chem. Phys. 111 (1999) 8088.
[26] F. Zaera, C.S. Gopinath, Chem. Phys. Lett. 332 (2000) 209.
[27] C.S. Gopinath, F. Zaera, J. Phys. Chem. B 104 (2000) 3194.
[28] F. Zaera, S. Wehner, C.S. Gopinath, J.L. Sales, V. Gargiulo, G. Zgrablich, J. Phys. Chem. B 105 (2001) 7771.
[29] V. Bustos, C.S. Gopinath, R. Uñac, F. Zaera, G. Zgrablich, J. Chem. Phys. 114 (2001) 10927.

[30] F. Zaera, C.S. Gopinath, J. Chem. Phys. 116 (2002) 1128.
[31] F. Zaera, C.S. Gopinath, Phys. Chem. Chem. Phys. 5 (2003) 646.
[32] L.A. Avalos, V. Bustos, R. Uñac, F. Zaera, G. Zgrablich, J. Mol. Catal. A 228 (2005) 89.
[33] H.J. Borg, J.F.C.-J.M. Reijerse, R.A. van Santen, J.W. Niemantsverdriet, J. Chem. Phys. 101 (1994) 10052.
[34] S.J. Alas, S. Cordero, I. Kornhauser, G. Zgrablich, J. Chem. Phys. 122 (2005) 144705.
[35] S.J. Alas, F. Rojas, I. Kornhauser, G. Zgrablich, J. Mol. Catal. A 244 (2006) 183.
[36] S.J. Alas, G. Zgrablich, J. Phys. Chem. B 110 (2006) 9499.
[37] D. Mei, Q. Ge, M. Neurock, L. Kieken, J. Lerou. Mol. Phys. 102 (2004) 361.
[38] M. Neurock, S.A. Wasileski, D. Mei, Chem. Eng. Sci. 59 (2004) 4703.
[39] R.J. Behm, P.A. Thiel, P.R. Norton, G. Ertl, J. Chem. Phys. 78 (1983) 7437;
R.J. Behm, P.A. Thiel, P.R. Norton, G. Ertl, J. Chem. Phys. 78 (1983) 7448.
[40] M.A. Barteau, E.I. Ko, R.J. Madix, Surf. Sci. 102 (1981) 99.
[41] K. Mase, Y. Murata, Surf. Sci. 277 (1992) 97.
[42] Y.Y. Yeo, L. Vattuone, D.A. King, J. Chem. Phys. 104 (1996) 3810.
[43] P.R. Norton, K. Griffiths, P.E. Binder, Surf. Sci. 138 (1984) 125.
[44] J.V. Barth, Surf. Sci. Rep. 40 (2000) 75.
[45] M. Rafti, J.L. Vicente, H. Uecker, R. Imbihl, Chem. Phys. Lett. 421 (2006) 577.
[46] M. Tammaro, J.W. Evans, J. Chem. Phys. 108 (1998) 7795.
[47] N.G. van Kampen, Stochastic Processes in Physics and Chemistry, Amsterdam, North-Holland, 1992.